

# Local RBF collocation method for Darcy flow

G. Kosec<sup>1</sup> and B. Šarler<sup>1</sup>

**Abstract** This paper explores the application of the mesh-free Local Radial Basis Function Collocation Method (LRBFCM) in solution of coupled heat transfer and fluid flow problems in Darcy porous media. The involved temperature, velocity and pressure fields are represented on overlapping sub-domains through collocation by using multiquadrics Radial Basis Functions (RBF). The involved first and second derivatives of the fields are calculated from the respective derivatives of the RBF's. The energy and momentum equations are solved through explicit time stepping. The pressure-velocity coupling is calculated iteratively, with pressure correction, predicted from the local continuity equation violation. This formulation does not require solution of pressure Poisson or pressure correction Poisson equations and thus much simplifies the Kassab and Divo formulation [Divo and Kassab (2007)]. The solution procedure is represented for a steady natural convection problem in a rectangular cavity, filled with Darcy porous media. The numerical examples include studies with different uniform discretization for differentially heated boundaries at filtration Rayleigh numbers  $Ra_F = 25, 50, 10^2, 10^3, 10^4$ , and aspect ratios  $A = 1/2, 1, 2$ . The solution is assessed by comparison with reference results of the fine mesh finite volume method (FVM) in terms of mid-plane velocities, mid-plane and insulated surface temperatures, mid-point streamfunction and Nusselt number. The advantages of the method are simplicity, accuracy and straightforward applicability in non-uniform node arrangements.

**keyword:** Darcy flow, primitive variables, natural convection, pressure-velocity coupling, meshless methods, local radial basis function collocation method, multiquadrics.

## 1 Introduction

Understanding of transport phenomena in the porous media is of great importance in science and engineering. Ever since the original work of [Darcy (1856)], these phenomena have been studied both experimentally and theoretically [Sahimi (1995)]. Despite the development of very sophisticated and relevant analytical techniques [Raghavan and Ozkan (1992)] a great majority of porous media models could be solved only by using discrete approximate solutions. These solutions in parallel with the development of computers nowadays allow the evaluation of physically very complex situations. However, the diversity of the involved length scales, inhomogeneities, and anisotropies, together with the justification of using different classical models (Darcy, Brinkman, Forchheimer) in a specific situation still represents a largely unresolved problem. An elaboration of the state-of-the-art in respective theoretical, experimental, and computational developments can be found in the comprehensive book [Kaviany (1995)]. A frequently encountered physical situation is the porous media natural convection problem, extensively treated by [Nield and Bejan (1999)]. The problem of natural convection in porous media was first studied by [Chan, Ivey and Barry (1994)] by using the Finite Difference Method (FDM). A similar study was performed approximately a decade ago by [Hickox and Gartling (1981)] by using the Finite Element Method (FEM). [Prasad and Kulacky (1984)] pioneered the use of the Finite Volume Method (FVM) for solving this problem. [Jecl, Škerget and Petrešin (2001)] were the first to solve the problem by the Boundary Domain Integral Method (BDIM). In recent years, a number of mesh-free methods [Atluri and Shen (2002), Atluri (2004), Liu (2003), Liu and Gu (2005)] have been developed to circumvent the problem of polygonisation encountered in the mentioned methods. In mesh-free methods,

---

<sup>1</sup> Laboratory for Multiphase Processes, University of Nova Gorica, Nova Gorica, Slovenia

approximation is constructed entirely in terms of a set of nodes. A class of such methods is based on collocation with radial basis functions [Šarler (2007)]. These functions [Buhmann (2000)] have been first under intensive research in multivariate data and function interpolation [Franke (1982)]. Kansa used them for scattered data approximation [Kansa (1990a)] and then for solution of PDEs [Kansa (1990b)]. The key point of the Radial Basis Function Collocation Method (RBF-CM) or Kansa Method (KM) for solving the PDEs is the approximation of the fields on the boundary and in the domain by a set of global approximation functions. The discretization is, respectively, represented only by grid-points (poles of the global approximation functions) in contrast to FEM, FVM, BDIM methods where appropriate polygonisation needs to be generated in addition, or FDM, where points are constrained to the coordinate lines. The main advantage of using the RBF-CM for solution of partial differential equations is its simplicity, applicability to different PDEs, and effectiveness in dealing with arbitrarily dimension and complicated domains. The method recently started to be applied in many scientific and engineering disciplines. It has been first used in the heat transport context by [Zerroukat, Power and Chen (1998)]. The method has been applied to the classical De Vahl Davis natural convection problem by asymmetric collocation in [Šarler, Perko, Chen and Kuhn (2001)] and by the symmetric and modified collocation in [Šarler (2005)]. The main disadvantage of the mentioned method represent the related full matrices that are very sensitive to the choice of the free parameter in RBFs and are difficult to solve for problems of the order of  $10^3$  unknowns or larger. The solution of related problem has been attempted by domain decomposition [Mai-Duy and Tran-Cong (2002)], multi-grid approach and compactly supported RBFs [Chen, Ganesh, Golberg and Cheng (2002)] which all represent a substantial complication of the original simple method. The radial basis functions have been first put into context of porous media flow by [Šarler, Gobin, Goyeau, Perko and Power (2000)] where the natural convection problem in Darcy porous media, and later Darcy-Brinkman porous media [Šarler, Perko, Gobin, Goyeau and Power (2004)] have been solved by the dual reciprocity boundary element method (DRBEM). This method belongs to the semi-mesh-free methods, because the domain fields are approximated by the global interpolation with the RBFs and the boundary fields by the boundary elements (polygons). The truly mesh-free RBF-CM has been for the

first time used for solution of Darcy porous media in [Šarler, Perko and Chen (2004)]. A substantial breakthrough in the development of the RBF-CM was its local formulation LRBFCM. This formulation was first developed for diffusion problems [Šarler and Vertnik (2006)], then to convection-diffusion problems with phase-change [Vertnik and Šarler (2006)], to industrial application of continuous casting [Vertnik, Založnik and Šarler (2006)], to solid-solid phase transformations [Kovačević and Šarler (2005)] and to solution of Navier Stokes equations [Chantasiriwan (2006), Divo and Kassab (2007)]. A similar local quadrature based RBF approach was developed by [Mai-Duy, Mai-Cao and Tran-Cong (2005), Shu, Ding and Yeo (2005)]. The RBFs can be used in solution of the solid mechanics problems [Le, Mai-Duy, Tran-Cong and Baker (2007), Mai-Duy, Khennane and Tran-Cong (2007)] as well. The main issue of the local version of the RBF-CM is the collocation on a sub-set of, in general, overlapping sub-domains, which drastically reduces the collocation matrix size on the expense of solving many small matrices instead of a large one. Since the method does not experience significant accuracy drawback in comparison with the global one, it represents a practical choice also for solving very large problems. The pressure correction algorithm, used by Divo and Kassab has been substantially simplified in [Kosec and Šarler (2007)]. This algorithm is in the present paper tested for solution of the Darcy natural convection in porous media. The main incitement of the present research was the extension of the LRBFCM method to physically new situations and testing of the new pressure correction algorithm for Darcy porous media flow with the slip boundary conditions.

## 2 Governing equations

The steady-state problem of the natural convection problem in the Darcy medium is described with following system of equations

$$\nabla \cdot \mathbf{v} = 0 \quad (1)$$

$$\nabla P = -\frac{\mu}{K} \mathbf{v} + \mathbf{f} \quad (2)$$

$$\nabla \cdot (\rho c_p T \mathbf{v}) = \nabla \cdot (\lambda \nabla T) \quad (3)$$

$$\mathbf{f} = \rho(T) \mathbf{g} \quad ; \quad \rho(T) = [1 - \beta_B (T - T_{\text{ref}})] \rho_0 \quad (4)$$

with  $\mathbf{v}$ ,  $P$ ,  $T$ ,  $\lambda$ ,  $c_p$ ,  $\mathbf{g}$ ,  $\rho_0$ ,  $\beta_B$ ,  $T_{\text{ref}}$ ,  $K$  and  $\mathbf{f}$  standing for Darcy velocity, pressure, temperature, thermal conductivity, specific heat, gravitational acceleration, density, coefficient of thermal expansion, reference

temperature for Boussinesq approximation, permeability and body force, respectively. The problem is solved on a fixed domain  $\Omega$  with boundary  $\Gamma$  where Dirichlet and Neumann boundary conditions for temperature and non-permeable conditions for velocity are used. The steady-state solution for different cavity aspect ratios and different filtration Rayleigh numbers is sought.

### 3 Solution procedure

In order to solve the problem, the time dependent variant of equations (2) and (3) is employed. The explicit time scheme is adopted to calculate the time derivative. To couple the momentum equation (2) with the mass continuity equation (1) the local pressure velocity coupling algorithm is used where the pressure correction is predicted from the mass continuity violation. In the first step, the velocity is estimated from the discretized form of equation (2)

$$\hat{\mathbf{v}} = \mathbf{v}_0 + \frac{\Delta t}{\rho_0 a_c} \left[ -\nabla P_0 - \frac{\mu}{K} \mathbf{v}_0 + \rho(T)\mathbf{g} \right] \quad (5)$$

where  $\hat{\mathbf{v}}$  denotes velocity at time  $t_0 + \Delta t$ ,  $\mathbf{v}_0$ ,  $P_0$  denotes velocity and pressure at time  $t_0$  and  $\Delta t$  denotes time-step. The  $a_c$  denotes acceleration coefficient, needed in order to pose a time-dependent Darcy equation as suggested in [Nield and Bejan (1999)]. The acceleration coefficient is set to unity in all numerical cases. The calculated velocity  $\hat{\mathbf{v}}$  does not satisfy the mass continuity equation in general and therefore a velocity correction  $\check{\mathbf{v}}$  has to be added in a sense that the mass continuity holds

$$\nabla \cdot (\hat{\mathbf{v}} + \check{\mathbf{v}}) = 0 \quad (6)$$

It is assumed that the velocity correction is affected only by the effect of the pressure correction

$$\check{\mathbf{v}} = -\frac{\Delta t}{\rho_0 a_c} \nabla \check{P} \quad (7)$$

where  $\check{P}$  stands for the pressure correction. By applying the divergence to the equation (7) one gets pressure correction Poisson equation.

$$\nabla \cdot \check{\mathbf{v}} = -\frac{\Delta t}{\rho_0 a_c} \nabla^2 \check{P} \quad (8)$$

Poisson equation (8) can be solved with proper pressure correction boundary conditions [Divo and Kassab (2007)]. Instead of solving the Poisson equation, an important assumption is adopted, as follows. The pressure correction is assumed to be linearly related to the Laplace of pressure correction. This assumption forms a basis for

iteration used to project the velocity into the divergence-free space. The iteration begins by setting the initial values to

$$\mathbf{v}^m = \hat{\mathbf{v}}, \quad P^m = P_0 \quad ; m = 1, \quad (9)$$

where  $m$  stands for the iteration index. In the second step, the pressure correction is calculated using the assumption of linearly correlated Laplace of pressure correction and pressure correction

$$\check{P} \approx L^2 \nabla^2 \check{P} = L^2 \frac{\rho_0}{\Delta t} \nabla \cdot \mathbf{v}^m \quad (10)$$

where  $L$  stands for characteristic length. In the third step, the intermediate pressure and velocity are corrected as

$$P^{m+1} = P^m + \beta \check{P} \quad (11)$$

$$\mathbf{v}^{m+1} = \mathbf{v}^m - \beta \frac{\Delta t}{\rho_0 a_c} \nabla \check{P} \quad (12)$$

where  $\beta$  stands for the relaxation parameter. If the mass conservation criteria

$$\nabla \cdot \mathbf{v}^{m+1} < \varepsilon_v \quad (13)$$

is not met than the iteration returns back to the equation (10), else pressure-velocity iteration is completed and the calculation proceeds to the next step. In the fourth step, the time dependent variant of energy equation is solved

$$T = T_0 + \frac{\Delta t}{\rho_0 c_p} \left[ \nabla \cdot (\lambda \nabla T_0) - \nabla \cdot (\rho_0 c_p T_0 \mathbf{v}_0) \right] \quad (14)$$

where  $T_0$  and  $T$  denote temperature at time levels  $t_0$  and  $t_0 + \Delta t$ . The steady-state is achieved when the criteria

$$\frac{|T - T_0|}{|T_0|} < \varepsilon_T \quad ; T_0 \neq 0 \quad (15)$$

$$T < \varepsilon_T \quad ; T_0 = 0$$

is met. If the criteria (15) is not met, the body force is updated and calculation returns back to the equation (5). The simulation flowchart is represented in Figure 1.

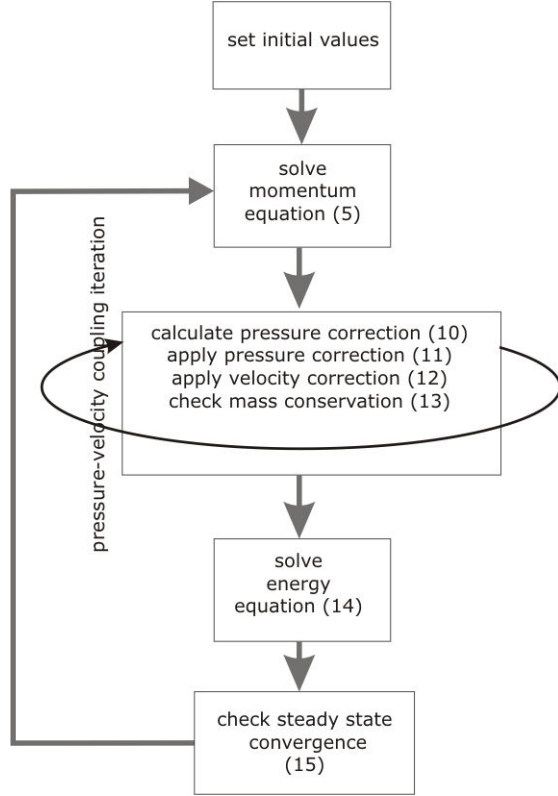


Figure 1: The calculation flowchart

#### 4 Radial basis function collocation method

The pressure, velocity and temperature fields are interpolated on the same grid points by LRBFCM where Hardy's multiquadrics are used as basis functions. The arbitrary function  $\theta$  is represented on a local sub-domain (Figure 2) as

$$\theta(\mathbf{p}) \approx \sum_{n=1}^N \alpha_n \Lambda_n(\mathbf{p}) \quad (16)$$

with  $\mathbf{p}$ ,  $\Lambda_n$ ,  $\alpha_n$  and  $N$  standing for position vector, basis function, collocation coefficient and number of collocation points, respectively. Hardy's multiquadrics basis functions are defined as

$$\Lambda_n(\mathbf{p}) = \sqrt{r_n^2(\mathbf{p}) + c^2 r_0^2}; \quad r_n^2 = (\mathbf{p} - \mathbf{p}_n) \cdot (\mathbf{p} - \mathbf{p}_n) \quad (17)$$

where  $c$  represents a dimensionless shape parameter. The scaling parameter  $r_0^2$  is set to the maximum nodal distance in the local sub-domain. The collocation coefficients are obtained from a collocation condition in the nodal points where equation (16) holds. In case when the number of nodes is the same as the number of the terms in the series (16), the system simplifies to

$$\theta(\mathbf{p}_i) = \theta_i = \sum_{n=1}^N \alpha_n \Lambda_n(\mathbf{p}_i) \quad (18)$$

$$\begin{bmatrix} \Lambda_{11} & \dots & \Lambda_{1N} \\ \dots & \dots & \dots \\ \Lambda_{M1} & \dots & \Lambda_{MN} \end{bmatrix} \begin{bmatrix} \alpha_1 \\ \dots \\ \alpha_N \end{bmatrix} = \begin{bmatrix} \theta_1 \\ \dots \\ \theta_N \end{bmatrix} \quad (19)$$

where  $\Lambda_{ni} = \Lambda_n(\mathbf{p}_i)$ . The collocation coefficients  $\alpha_n$  are obtained by solving the system (19). The spatial derivatives of the function  $\theta$  can be easily obtained through

$$\frac{\partial}{\partial p_\sigma} \theta(\mathbf{p}) \approx \sum_{n=1}^N \alpha_n \frac{\partial}{\partial p_\sigma} \Lambda_n(\mathbf{p}) \quad (20)$$

$$\frac{\partial^2}{\partial^2 p_\sigma} \theta(\mathbf{p}) \approx \sum_{n=1}^N \alpha_n \frac{\partial^2}{\partial^2 p_\sigma} \Lambda_n(\mathbf{p}) \quad (21)$$

where  $p_{\sigma=x,y}$  stand for Cartesian coordinates. All necessary derivatives to construct the involved divergence, gradient and Laplace operators can be calculated from equations (20) and (21). The integral of function  $\theta$  over  $p_\sigma$  (needed in the calculation of the streamfunction) can be evaluated as well

$$\int \theta(\mathbf{p}) dp_\sigma = \sum_{n=1}^N \alpha_n \int \Lambda_n(\mathbf{p}) dp_\sigma \quad (22)$$

In this paper only the simplest local sub-domain of five collocation points is used with the overlapping collocation sub-domain strategy (Figure 2). The points denoted with cross over the circle are the points where values of interest are calculated. At the interior points the derivatives are calculated at the central sub-domain points while at the boundary points with Neumann boundary condition the values of function are calculated. At the boundary collocation points with the Neumann boundary conditions the derivative instead of the function value is known. In such points the equation (18) is replaced with

$$\frac{\partial}{\partial p_\sigma} \theta(\mathbf{p}_i) = \sum_{n=1}^N \alpha_n \frac{\partial}{\partial p_\sigma} \Lambda_n(\mathbf{p}_i) \quad (23)$$

where index  $i$  stands for index of a point where the derivative is known. The overlapping sub-domain strategy is schematically represented for two neighboring interior points in Figure 2, as well. All interior points at time level  $t_0 + \Delta t$  are evaluated first. Afterwards, the calculation continues with the Neumann boundary points at time level  $t_0 + \Delta t$ . The five pointed local sub-domain strategy is used to solve all cases. The convergence with respect to the sub-domain selection has been studied in our previous work [Šarler and Vertnik (2006)], where the results with five- and nine-point sub-domains were compared for diffusion problems. These results do not differ much (the relative difference is below 0.1%), but the implementation on the boundary is much more complex and less stable,

therefore only the simplest five-noded sub-domain has been used in the present work.

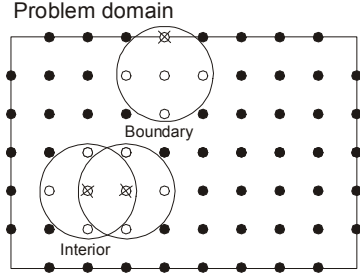


**Figure 2:** Five-noded collocation sub-domain and total space discretization schematics

## 5 Numerical examples

The natural convection in a rectangular enclosure is taken as a benchmark due to its well known solution. The vertical walls are differentially heated while horizontal walls are isolated. All walls are non-permeable and due to Darcy's law the slip boundary condition applies. The normal velocity is zero (Figure 3).

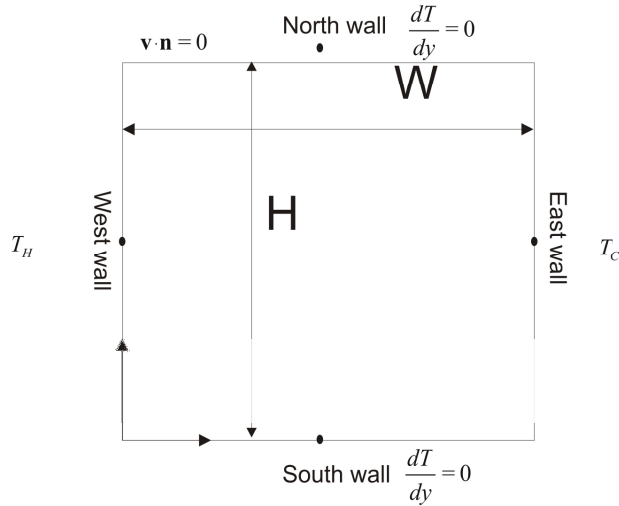


**Figure 3:** The problem domain

All results are stated in Cartesian coordinates and standard dimensionless form

$$x = \frac{\bar{x}}{W} \quad y = \frac{\bar{y}}{W} \quad u = \frac{\bar{u}L\rho c_p}{\lambda} \quad v = \frac{\bar{v}L\rho c_p}{\lambda} \quad (24)$$

$$\tau = \frac{T - T_C}{T_H - T_C}$$

where  $x, y$  stand for dimensionless coordinates,  $u, v$  stand for dimensionless horizontal and vertical velocity components, and  $\tau$  stands for dimensionless temperature. Filtration Rayleigh number is defined as

$$Ra_F = \frac{\rho^2 c_p K g \beta (T_H - T_C) B}{\lambda \mu} \quad (25)$$

Nusselt number is calculated by equation

$$Nu(x, y) = -\frac{\partial \tau(x, y)}{\partial x} + u(x, y)\tau(x, y) \quad (26)$$

and the streamfunction is calculated by integrating a velocity component

$$\psi(x, y) = \int_{H=0}^y u(x, y') dy' \quad (27)$$

Three different cavity height-width aspect ratios were tested ( $A = H/W$ ),  $A = 0.5$ ,  $A = 1$  and  $A = 2$  for filtration Rayleigh numbers up to  $10^4$ . The results were compared with (a) [Šarler, Gobin, Goyeau, Perko and Power (2000)], (b) [Ni and Beckermann (1991)], and (c) [Prax, Sadat and Salagnac (1996)] where good agreement was achieved (Table 1). The streamlines and temperature contour plots of the present work are shown in Figures 4-11. The temperature contour step is for all cases 0.005 while streamline step varies (from 0.5 for  $Ra_F = 50$  to 5 for  $Ra_F = 10^4$ ) in the tackled cases.

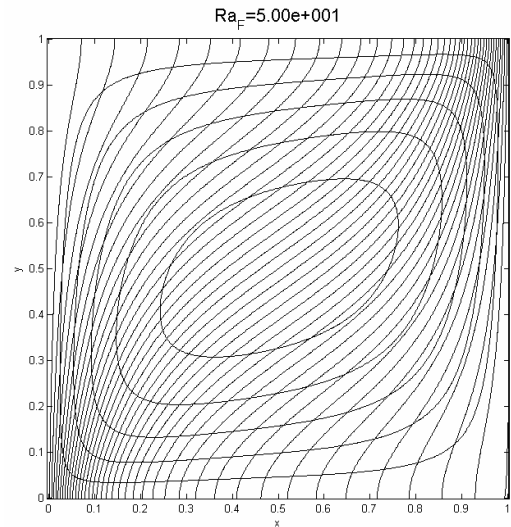


**Figure 4:** Temperature contour plot and streamlines for  $A = 1$ ,  $Ra_F = 50$

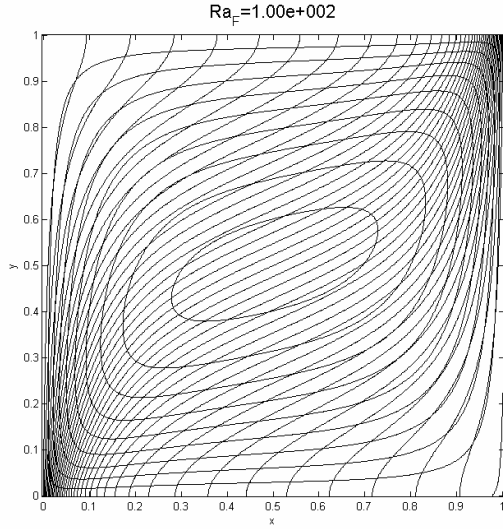


**Figure 5:** Temperature contour plot and streamlines for  $A = 1$ ,  $Ra_F = 100$

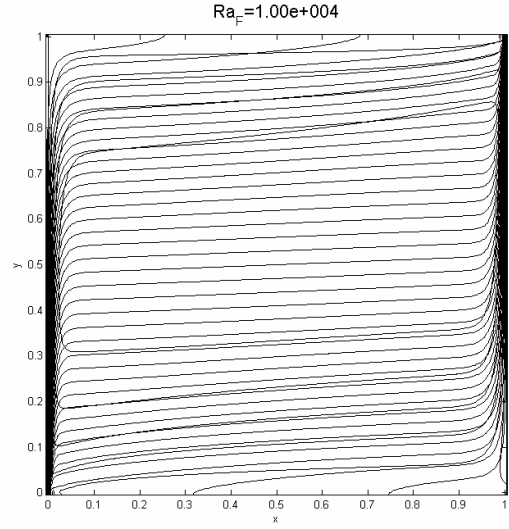


**Figure 7:** Temperature contour plot and streamlines for  $A = 1$ ,  $Ra_F = 10^4$

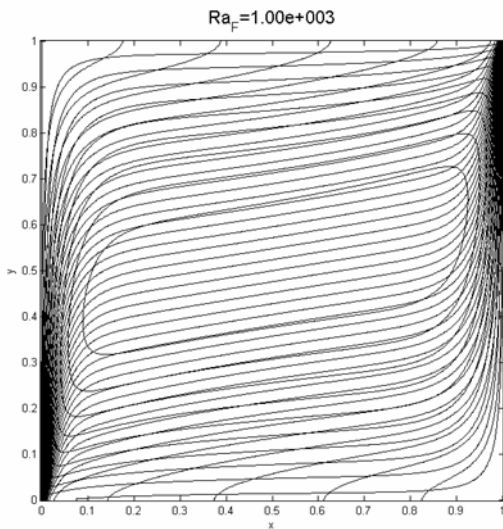


**Figure 6:** Temperature contour plot and streamlines for  $A = 1$ ,  $Ra_F = 10^3$

Additional result comparison with reference FVM solution, previously used in [Šarler, Gobin, Goyeau, Perko and Power (2000)], for mid-plane velocities (Figure 12), hot-side Nusselt number (Figure 13), mid-plane and top temperature profiles (Figure 14) is done for case with  $A = 1$  and filtration Rayleigh number  $Ra_F = 100$ .

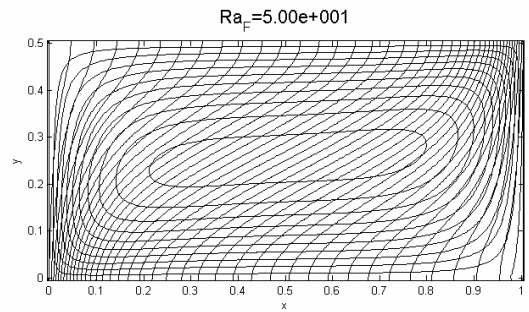


**Figure 8:** Temperature contour plot and streamlines for  $A = 1/2$ ,  $Ra_F = 50$

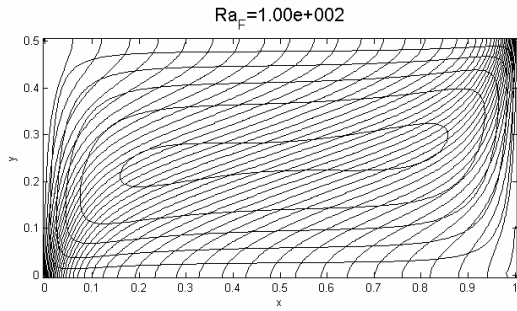


Figure 9: Temperature contour plot and streamlines for  $A = 1/2$ ,  $Ra_F = 100$

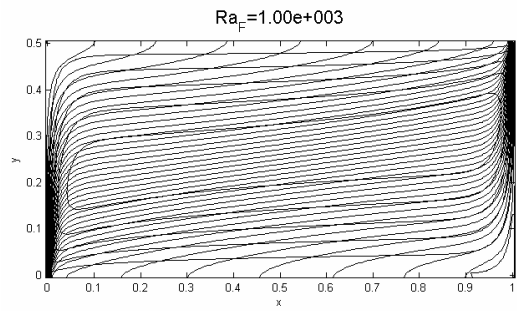


Figure 10: Temperature contour plot and streamlines for  $A = 1/2$ ,  $Ra_F = 10^3$

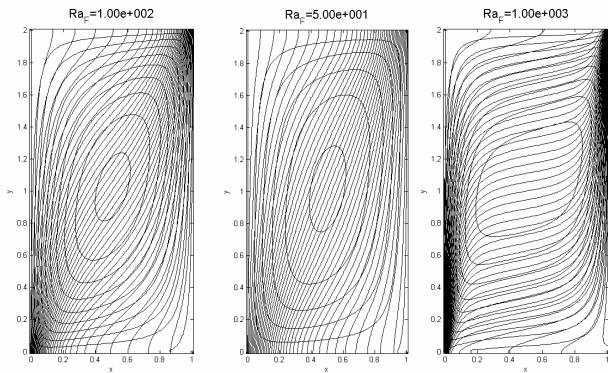


Figure 11: Temperature contour plot and streamlines for  $A = 2$ ,  $Ra_F = 50, 100$ , and  $10^3$

Table 1: Comparison of the results

$Ra_F$	$A$	$v_{max}$	$u_{max}$	$\overline{Nu}$	$\psi_{mid}$	ref/ discretization
50	1			1.979	2.863	(a)
		18.112	11.174	1.941	2.860	101x101
		17.928	11.214	1.962	2.853	201x201
		17.845	11.236	1.975	2.848	401x401
$10^2$	1	35.889	17.380	3.101	4.375	(a)
				3.103		(b)
				3.010		(c)
		37.454	17.500	3.040	4.510	101x101
		37.055	17.562	3.071	4.607	201x201
		36.873	17.603	3.086	4.655	401x401
$10^3$	1			13.42		(b)
		441.771	72.560	13.044	17.062	101x101
		435.107	74.741	13.455	18.791	201x201
$10^4$	1	4946.968	257.394	36.720	35.436	101x101
		4880.108	287.375	44.295	49.235	201x201
		4880.197	287.375	44.295	49.310	401x401
50	0.5			2.135	2.148	(a)
		23.402	16.562	2.130	2.090	101x201
$10^2$	0.5	52.136	27.109	3.720	3.509	101x201
$10^3$	0.5	732.806	120.724	22.452	15.928	101x201
50	2			1.386	2.639	(a)
		11.710	7.039	1.367	2.608	201x101
$10^2$	2	23.283	10.779	11.944	4.630	201x101
$10^3$	2	241.218	45.111	7.250	19.576	201x101

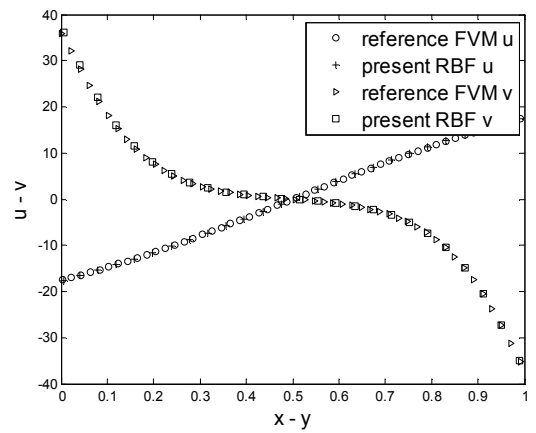
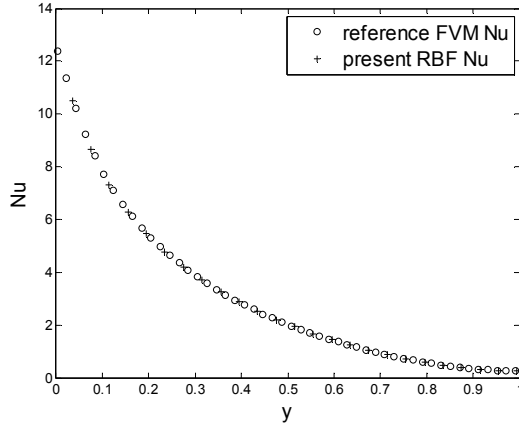
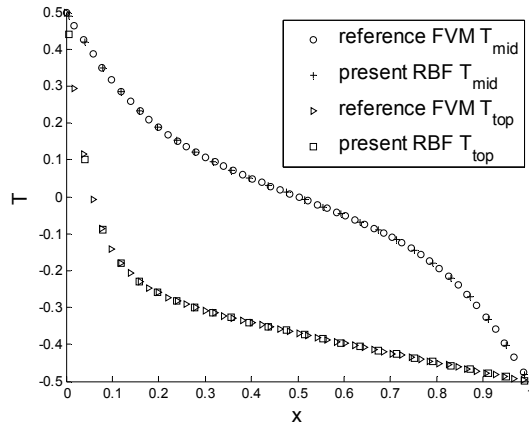


Figure 12: Mid-plane velocities comparison with reference FVM solution



**Figure 13:** Hot-side Nusselt number comparison with reference FVM solution



**Figure 14:** Mid-plane and top temperature profiles comparison with reference FVM solution

## 6 Numerical implementation and result discussion

All numerical procedures are written in C++ language and compiled with Intel C++ compiler 9.1. The LAPACK routines are used to solve the LU decomposition. All calculations are done with Intel Xeon processor with 4 CPU cores. The results for low filtration Rayleigh numbers agree well with other works. In addition to previously treated cases in quoted works, results for  $Ra_F = 10^3$  and  $Ra_F = 10^4$  are represented in this work. The pressure-velocity coupling algorithm was tested for up to  $400 \times 400$  uniformly distributed nodes and it behaves convergent. The initial fields have been set to zero in all calculations. The time step and pressure-velocity iteration criteria is stated in (Table 2) for all calculated cases. For all cases the relaxation parameter  $\beta$

has been set to the same numeric value as the time step. The RBF free parameter in equation (17) was found to give best results around  $c = 30$ . All calculations require less than an hour of CPU time to reach the steady-state, where the steady-state criteria  $\varepsilon_T < 10^{-5}$  is used in all cases.

**Table 2:** Pressure-velocity iteration criteria  $\varepsilon_v$  and time-step  $\Delta t$ .

Ra	A	$\varepsilon_v$	$\Delta t$	discr.
50	1	0.01	1e-04	100×100
10 <sup>2</sup>	1	0.1	1e-04	100×100
10 <sup>3</sup>	1	1	1e-04	100×100
10 <sup>4</sup>	1	1	5e-06	100×100
50	2	0.1	1e-05	200×100
10 <sup>2</sup>	2	1	1e-05	200×100
10 <sup>3</sup>	2	1	1e-05	200×100
50	0.5	0.1	1e-04	100×200
10 <sup>2</sup>	0.5	1	1e-05	100×200
10 <sup>3</sup>	0.5	1	1e-05	100×200

## 7 Conclusions

This paper describes the initial attempts at solving the problem of Darcy natural convection in porous media by the LRBFCM. Results are obtained for rectangular cavities with aspect ratio 0.5, 1 and 2, and filtration Rayleigh numbers 50, 10<sup>2</sup>, 10<sup>3</sup> and 10<sup>4</sup>. The method is structured on the local version of the Hardy's multiquadrics. The main advantage of the method represents the polygon-free discretization, simple numerical implementation, which is very similar in 2D and 3D problems, and no numerical integration involved. Present work employs a new, entirely local approach, for solving the pressure-velocity coupling without the need to solve the pressure Poisson or pressure Poisson correction equations. It was successfully tested for Darcy porous media flow. The algorithm is simple to implement and it needs a small number of operations per iteration cycle. The solver is completely explicit and therefore it is trivial to parallelize it. The method is potentially competitive because of the obvious man-power reduction in grid generation. The developed method represents a substantial step forward with respect to the global RBFMC [Šarler, Perko and Chen (2004)] one, because of its capabilities to solve problems with large degree of

unknowns. Further investigations follow in the optimum relaxation parameter analysis, the time-dependent and non-uniform [Perko and Šarler (2007)] nodes configuration, and testing of the algorithm in more complex physical situations (solidification, multi layer domains, more complex geometries, ...).

#### Acknowledgment:

The authors would like to express their gratitude to Slovenian Research Agency for support in the framework of the projects Young Researcher Program 1000-06-310232 (G.K.), J2-6403 and L9-9508 (B.Š.).

#### 8 References

**Atluri, S .N.; Shen, S.** (2002): *The Meshless Method*, Tech Science Press, Encino.

**Atluri, S.N.** (2004): *The Meshless Method (MLPG) for Domain and BIE Discretization*, Tech Science Press, Forsyth.

**Buhmann, M.D.** (2000): *Radial Basis Functions*, Cambridge University Press, Cambridge.

**Chan, B. K. C.; Ivey, C. M.; Barry, J.M.** (1994): Natural convection in enclosed porous media with rectangular boundaries. *Wärme Stoffübertragung*, vol. 7, pp. 22–30.

**Chantasiriwan, S.** (2006): Performance of Multiquadric Collocation Method in Solving Lid-driven Cavity Flow Problem with Low Reynolds Number *CMES*, vol. 15, pp. 137-146.

**Chen, C. S.; Ganesh, M.; Golberg, M. A.; Cheng, A. H. D.** (2002): Multilevel compact radial basis functions based computational scheme for some elliptic problems. *Computers and Mathematics with Applications*, vol. 43, pp. 359-378.

**Darcy, H.** (1856): *Les fontaines publique de la Ville de Dijon*, Victor Delmont, Paris.

**Divo, E.; Kassab, A. J.** (2007): An efficient localized RBF meshless method for fluid flow and conjugate heat transfer. *ASME Journal of Heat Transfer*, vol. 129, pp. 124-136.

**Franke, J.** (1982): Scattered data interpolation: tests of some methods. *Mathematics of Computation*, vol. 48, pp. 181-200.

**Hickox, C.E.; Gartling, D.K.** (1981): A numerical study of natural convection in a horizontal porous layer subjected to an end-to-end temperature difference. *ASME Journal of Heat Transfer*, vol. 103, pp. 797–802.

**Jeel, R.; Škerget, L.; Petrešin, E.** (2001): Boundary domain integral method for transport phenomena in porous media. *International Journal for Numerical Methods in Fluids*, vol. 35, pp. 35–59.

**Kansa, E. J.** (1990a): Multiquadrics – a scattered data approximation scheme with application to computational fluid dynamics, part I. *Computers and Mathematics with Applications*, vol. 19, pp. 127-145.

**Kansa, E. J.** (1990b): Multiquadrics – a scattered data approximation scheme with application to computational fluid dynamics, part II. *Computers and Mathematics with Applications*, vol. 19, pp. 147-161.

**Kaviany, M.** (1995): *Principles of Heat Transfer in Porous Media*, Springer, Berlin.

**Kosec, G.; Šarler, B.** (2007): Solution of Thermo-Fluid Problems by Collocation with Local Pressure Correction. *International Journal of Numerical Methods for Heat and Fluid Flow*, (in press).

**Kovačević, I.; Šarler, B.** (2005): Solution of a phase-field model for dissolution of primary particles in binary aluminum alloys by an r-adaptive mesh-free method. *Materials Science and Engineering A*, vol. 413–414, pp. 423–428.

**Le, P.; Mai-Duy, N.; Tran-Cong, T.; Baker, and G.** (2007): A Numerical Study of Strain Localization in Elasto-Thermo-Viscoplastic Materials using Radial Basis Function Networks *CMC*, vol. 5, pp. 129-150.

**Liu, G.R.** (2003): *Mesh Free Methods*, CRC Press, Boca Raton.

**Liu, G.R.; Gu, Y.T.** (2005): *An Introduction to Meshfree Methods and Their Programming*, Springer, Dordrecht.

**Mai-Duy, N.; Khennane, A.; Tran-Cong, and T.** (2007): Computation of Laminated Composite Plates using Integrated Radial Basis Function Networks *CMC*, vol. 5, pp. 63-78.

**Mai-Duy, N.; Mai-Cao, L.; Tran-Cong, and T.** (2005): Computation of transient viscous flows using indirect radial basis function networks *CMES*, vol. 129, pp. 124-136.

**Mai-Duy, N.; Tran-Cong, T.** (2002): Mesh-free radial basis function network methods with domain decomposition for approximation of functions and numerical solution of Poisson's equations. *Engineering Analysis with Boundary Elements*, vol. 26, pp. 133-156.

**Ni, J.; Beckermann, C.** (1991): Natural Convection in a Vertical Enclosure Filled with Anisotropic Porous Media. *ASME Journal of Heat Transfer*, vol. 113, pp. 1033-1037.

**Nield, D. A.; Bejan, A.** (1999): *Convection in Porous Media, Second Edition*, Springer, Berlin.

- Perko, J.; Šarler, B.** (2007): Weigh function shape parameter optimization in meshless methods for non-uniform grids. *CMES*, vol. 19, pp. 55-68.
- Prasad, V.; Kulacky, F.A.** (1984): Convective heat transfer in a rectangular porous cavity. Effect of aspect ratio on flow structure and heat transfer. *ASME Journal of Heat Transfer*, vol. 106, pp. 158-65.
- Prax, C.; Sadat, H.; Salagnac, P.** (1996): Diffuse Approximation method for Solving Natural Convection in Porous Media. *Transport in Porous Media*, vol. 22, pp. 215-223.
- Raghavan, R.; Ozkan, E. A.** (1992): Method for computing unsteady flows in porous media. *Pitman research notes in mathematics series*, vol. 318.
- Sahimi, M.** (1995): *Flow and Transport in Porous Media and Fractured Rock*, VCH Verlagsgesellschaft mbH, Weinheim.
- Shu, C.; Ding, H.; Yeo, K. S.** (2005): Computation of incompressible Navier-Stokes equations by local RBF-based differential quadrature method. *CMES*, vol. 7, pp. 195-205.
- Šarler, B.** (2005): A radial basis function collocation approach in computational fluid dynamics. *Computer Modelling in Engineering & Sciences*, vol. 7, pp. 185-193.
- Šarler, B.** (2007): From global to local radial basis function collocation method for transport phenomena, *Advances in Meshfree Techniques*, Springer, Berlin, pp. 257-282.
- Šarler, B.; Gobin, D.; Goyeau, B.; Perko, J.; Power, H.** (2000): Natural convection in porous media - dual reciprocity boundary element method solution of the Darcy model. *International Journal of Numerical Methods in Fluids*, vol. 33, pp. 279-312.
- Šarler, B.; Perko, J.; Chen, C. S.; Kuhn, G.** (2001): A meshless approach to natural convection, *International Conference on Computational Engineering and Sciences, CD proceedings*.
- Šarler, B.; Perko, J.; Chen, C.S.** (2004): Radial basis function collocation method solution of natural convection in porous Media. *International Journal of Numerical Methods for Heat & Fluid Flow*, vol. 14, pp. 187-212.
- Šarler, B.; Perko, J.; Gobin, D.; Goyeau, B.; Power, H.** (2004): Dual reciprocity boundary element method solution of natural convection in Darcy-Brinkman porous media. *Engineering Analysis with Boundary Elements*, vol. 28, pp. 23-41.
- Šarler, B.; Vertnik, R.** (2006): Meshfree explicit local radial basis function collocation method for diffusion problems. *Computers and Mathematics with Applications*, vol. 51, pp. 1269-1282.
- Vertnik, R.; Šarler, B.** (2006): Meshless local radial basis function collocation method for convective-diffusive solid-liquid phase change problems. *International Journal of Numerical Methods for Heat and Fluid Flow*, vol. 16, pp. 617-640.
- Vertnik, R.; Založnik, M.; Šarler, B.** (2006): Solution of transient direct-chill aluminium billet casting problem with simultaneous material and Interphase moving boundaries by a meshless method. *Engineering Analysis with Boundary Elements*, vol. 30, pp. 847-855.
- Zerroukat, M.; Power, H.; Chen, C.S.** (1998): A numerical method for heat transfer problems using collocation and radial basis functions. *International Journal of Numerical Methods in Engineering*, vol. 42, pp. 1263-1278.